Journal of Paleolimnology (2005) 34: 325–337
DOI 10.1007/s10933-005-5022-4

Environmental history of Lago di Tovel, Trento, Italy, revealed by sediment cores and 3.5 kHz seismic mapping

Thomas Kulbe[1,*], Flavio Anselmetti[2], Marco Cantonati[3] and Michael Sturm[1]
[1]*Swiss Federal Institute of Environmental Science and Technology (EAWAG), Überlandstrasse 133, CH-8600 Dübendorf, Switzerland;* [2]*Geological Institute ETH-Zürich, Sonneggstrasse 5, CH-8092 Zürich, Switzerland;* [3]*Museo Tridentino di Scienze Naturali, Limnology and Phycology Section, Via Calepina 14, I-38100 Trento, Italy; *Author for correspondence (e-mail: thomas.kulbe@eawag.ch)*

Received 13 November 2004; accepted in revised form 22 March 2005

Key words: Landslide, Mass movement, Mountain lake, Sediment distribution, Seismic survey

Abstract

Proxy data from a total of 30 sediment cores and information from a seismic survey show that the sedimentological and limnological history of Lago di Tovel (1178 m a.s.l.) has been significantly influenced by slope dynamics of its mountainous catchment. The lake represents a dead-ice lake with pro-glacial deposits at the base of its sedimentary record. A prominent lake level rise in 1597/1598 that increased maximum water depth from ~20 to 39 m caused slope instabilities, leading to the deposition of mass-flow sediments with a maximum thickness of 2.5 m in the northern part of the lake and less than 50 cm in the southern part, resulting in a total volume of more than 113,000 m^3. Consequently, a rough lake bottom morphology was produced, which led to distinct differences in sedimentation rates of 0.07 cm yr^{-1} on sills and 0.18 cm yr^{-1} within depressions. The age of the top of the mass-flow deposits was used to validate the ages of the younger, laminated sediments, which were dated by ^{210}Pb and ^{137}Cs. Lithological investigations showed that the sediments below the mass-flow deposits are also laminated and that they were not bioturbated. The long-term meromixis of Lago di Tovel is therefore mainly due to a combination of its topographic setting and the 5-month period of ice cover. Both prevent effective mixing of the lake by strong winds during spring and autumn. Distinct spatial differences in sediment distribution within the lake show that it is risky to interpret proxy data from only one coring site, even if the lake is very small. This is especially true in mountainous areas, where rock falls, mass movements, and slope instabilities of a significant size may have considerable effects on lakes.

Introduction

Mountain lakes are sensitive ecosystems that react fast and directly to environmental changes. The importance of mountain lakes and their sediment records for obtaining a better understanding of the causes and dimensions of past and recent climate change, and of the role played by anthropogenic influence, has been shown in several recent papers (Agustí-Panareda and Thompson 2002; Battarbee et al. 2002; Bradley et al. 2003; Ohlendorf et al. 2003; Sturm et al. 2003).

Lago di Tovel, one of the major attractions of the Adamello Brenta National Park, has been famous since the late 19th century. For almost 150 years an intense red color developed in the shallow part of the lake during summer (Freshfield 1875). However, this phenomenon ceased around 1964. Reddening of the lake water is caused by the carotenoid pigment Astaxanthin, produced by the

dinoflagellate *Glenodinium sanguineum* (described by Marchesoni 1941). The causes and conditions of the onset, development and disappearance of the reddening phenomenon are under discussion. Intense summer blooms of the red dinoflagellate species, the synthesis and accumulation of the carotenoid, as well as the regular north-eastern breeze that causes dinoflagellate cells to accumulate in the shallow bay, were the major requirements identified by Baldi (1941) for the occurrence of this phenomenon. All these aspects have been recently investigated (e.g., Cantonati et al. 2003). Various hypotheses have been advanced to explain the disappearance of the reddening phenomenon. Changes in the nutrient budget of the catchment and of the lake caused by cattle breeding altered the phosphorus input and changed the productivity of the lake and the availability of the main algal nutrients (P and N) at the time of the blooms (Perini Aregger 1968; Dodge 1970; Paganelli et al. 1980; Fuganti and Morteani 1999; Cantonati et al. 2003). Higher rainfall in spring and summer due to local conditions, global warming in combination with a decrease in rainfall in the Alps and pesticide input by atmospheric transport from the adjacent main valley are other scenarios proposed to explain a change in dinoflagellate production (Perini Aregger 1968; Dodge 1970; Paganelli et al. 1980; Fuganti and Morteani 1999; Cantonati et al. 2003).

The reddening of the lake, and in particular its cessation, is both of scientific and of social and economic (tourism) interest. Thus, in 2001, a project was initiated to investigate present and past conditions of the lake ecosystem in detail using biological, geochemical, mineralogical and sedimentological methods. The aim of this paper is to present the results of a study of the lake's post-glacial sedimentological history, emphasizing the relevance of the influence of dynamic slopes and the necessity of using data from several cores taken along transects for such studies in mountain lakes.

Lake characteristics

Lago di Tovel is situated at 1178 m a.s.l. in the Brenta Dolomites of the Italian Alps (46°15′40″ N, 10°49′40″ E, Figure 1) with dolomites and karstic limestones in its catchment. Lago di Tovel has a surface area of 382,000 m^2, a water volume of 7.4×10^6 m^3 and a maximum water depth of 39 m. Morphologically, the lake can be divided into a deep central basin (39 m), a small eastern basin separated from the main basin by a sill, and a shallow bay to the south-west, with a maximum depth of ~5 m, that dries out in winter. The lake is located in a Late Glacial landslide area and the lake basin is assumed to have been formed after the melting of dead-ice. Oetheimer (1992) states that a landslide dammed an ancient outlet and caused a lake level rise of 21 m in 1597/1598, which formed the modern lake. This event was dated from a rooted tree trunk found 18 m below the modern lake surface.

The bottom water of the lake is anoxic, partly because the mountainous surroundings prevent frequent mixing of the lake water by wind. The mixolimnion is weakly stratified from June to October and ice-covered from December to April. Lago di Tovel is classified as meromictic and oligotrophic with phosphorus as the limiting factor (Cordella et al. 1980; Paganelli et al. 1988). The lake water is supplied by surface inflow and by underwater springs. The lake level, which varies by up to 8 m, is low during winter and early spring, when the inflows are frozen, and is usually high in spring after snowmelt (Biondi et al. 1981; Lami et al. 1991; Paganelli 1992; Fuganti and Morteani 1999; Corradini et al. 2001).

Methods

Seismic surveys

In order to obtain information on basin morphology and on the thickness of unconsolidated sediments, and to find the best sampling sites for an undisturbed, continuous sediment sequence, detailed seismic mapping was carried out in October 2001. A high-resolution, single channel seismic survey with a 3.5 kHz pinger system (Geoacoustics) was conducted, using a rubber dinghy pushing a catamaran carrying the pinger source. A dense grid of 11 seismic lines resulting in ~8 km of seismic profiles allowed a quasi-3D architecture of the sedimentary basin-fill to be compiled (Figures 2 and 3). Precise positioning of the boat was achieved with a GPS. The shot interval was 300 milliseconds (ms). The seismic data were digitally recorded in SEG-Y format, then processed and interpreted in the laboratory

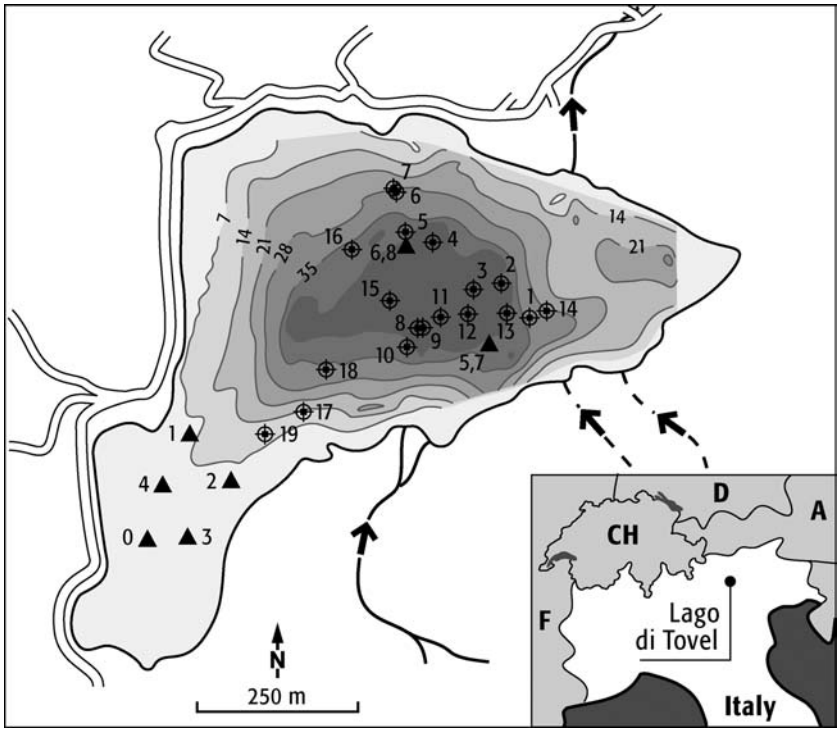

Figure 1. Bathymetry of Lago di Tovel (7 m contour interval, darkest color: 39.5 m) and coring locations. Sites cored in 2001 are shown as triangles and those cored in 2003 as open circles with a cross. Inflows and outflow: solid lines, permanent; dashed lines, temporary.

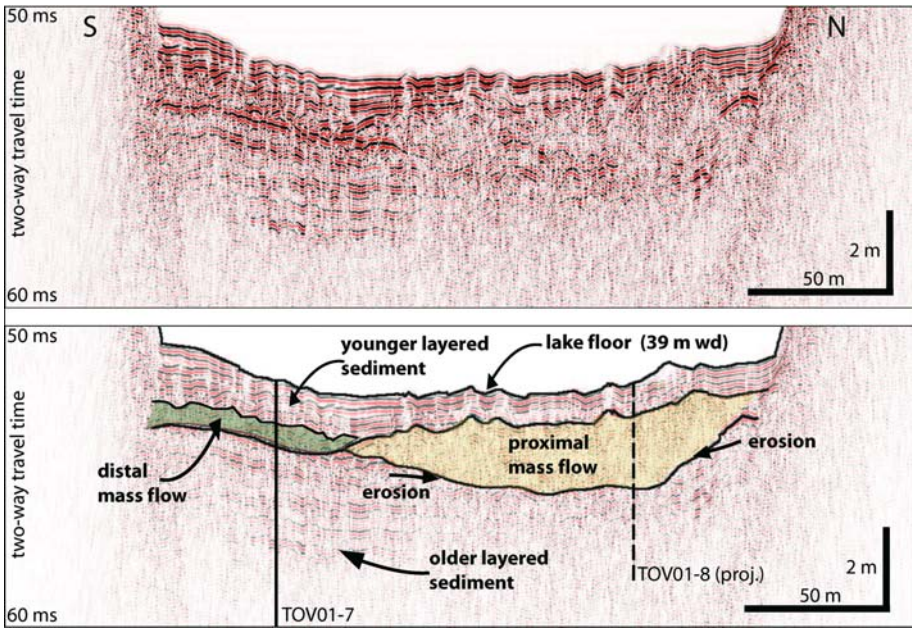

Figure 2. Seismic section Q5 crossing the lake in a N–S direction. Piston core TOV01-7 is located on this seismic line; piston core TOV01-8 is projected perpendicularly on to the seismic section. Note the different seismic facies of mass-flow deposits and regular bedded deposits, and the erosion and/or deformation at the base of the proximal (northern) mass-flow unit.

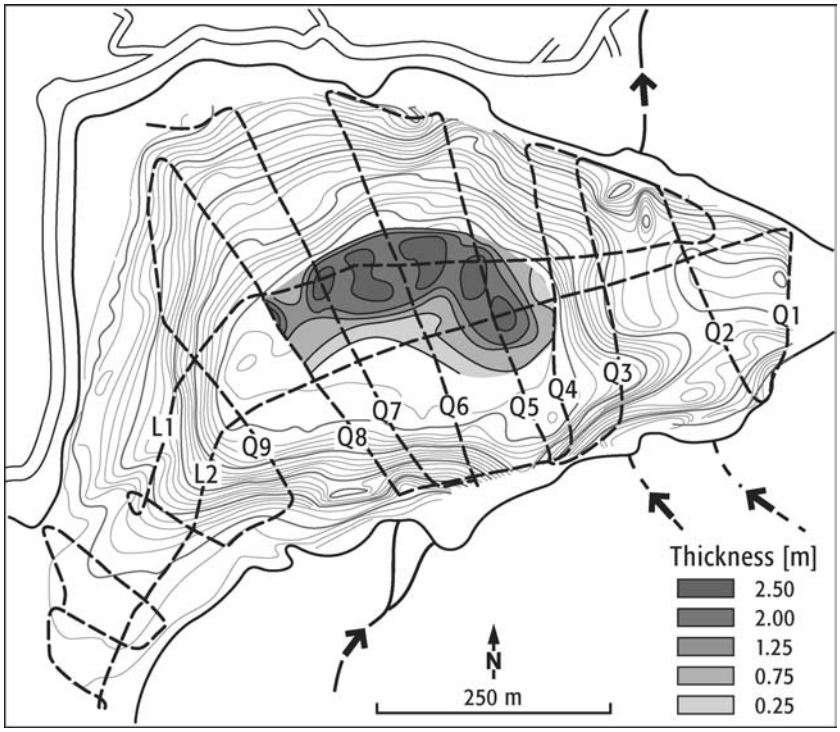

Figure 3. Seismic lines (dashed) and distribution and thickness of the slump of 1597/1598. Inflows and outflow: solid line, permanent; dashed line, temporary.

by SPW and KingdomSuite software. Constant shallow noises, caused by the vibrations of the pinger itself, were digitally subtracted from the signal. A bandpass filter (1400–6500 Hz) and an automatic gain control with window length of 50 ms were applied.

Coring and sampling

Based on the results of the seismic survey, the best sites were determined for taking short gravity cores and long piston cores (Figure 1). During two campaigns in 2001 and 2003 a total of 27 gravity cores were taken with a UWITEC gravity corer (8 kg weight and transparent PVC core liners of 63 mm diameter) and an EAWAG-63 gravity corer (30 kg weight and transparent PVC core liners of 63 mm diameter). Cores of length 10–22 cm were obtained from four stations in the shallow bay where the reddening had occurred in the past. Three cores (60–96.5 cm) were taken in an intermediate water depth and 20 gravity cores of 37–78 cm length were taken from the deep part of the lake. A total of three piston cores were taken from the central part of the lake, using a UWITEC piston corer (transparent PVC core liners of 63 mm diameter). One of the long core sites (TOV01-8, 490 cm) lay to the north of the central lake basin and two sites (TOV01-5, 721 cm, and TOV01-7, 734 cm) to its south. All cores were opened for lithological inspection and photographs. Based on the information thus obtained, several cores were sub-sampled at a resolution of 0.5 cm for the upper 20 cm and at 1-cm intervals below this. A multi-proxy approach was subsequently adopted (sedimentology, geochemistry, mineralogy) to characterize the sediments. Selected cores were sub-sampled for pollen, pigments and other biological parameters.

Physical properties

Physical sediment properties were measured on all cores longer than 50 cm using an automated 'Multi-Sensor Core Logger' (Geotek). This technique allows continuous, non-destructive

logging and measures P-wave velocity, bulk wet density, and magnetic susceptibility (Zolitschka et al. 2001). Physical properties can be used for both core-to-core correlation and down-core correlation of overlapping core sections.

Sedimentological, mineralogical, and geochemical methods

The water content was calculated on the basis of the difference in weight between the wet and dry samples. The density of the dry sediment was measured with a glass-pycnometer. A laser particle analyzer (Malvern Mastersizer) was used to determine the grain size distribution of the sediments < 150 μm. Prior to the measurements, samples ($\sim$40 mg) were suspended in 3 ml of 0.01% Calgon solution to avoid coagulation. The mineral composition of selected sediment samples was determined by X-ray diffraction using a Scintag XDS 2000 diffractometer at 45 kV and 40 mA with Cu Kα radiation between 4° and 70° (2θ), and the graphical analysis program MacDiff 4.2.5. Total carbon (TC) and total nitrogen (TN) content were measured with a Euro EA-CNS (Hekatech), which heats the samples to 1000° C. Subsequently, the gas is separated by an internal gas chromatographical system and determined by a sensitive heat-conductivity system. The total inorganic carbon (TIC) content of the sediment was analyzed by coulometry (UIC Coulometrics), in which each sample is treated with hot hydrochloric acid (2 mol l^{-1}) to convert the TIC portion into CO_2. The amount of total organic carbon (TOC) was calculated by subtracting the TIC aliquot from the TC content.

Dating

For dating, the ^{210}Pb and ^{137}Cs activities in the freeze-dried samples were measured in a well-type Geli detector for a minimum of 24 h by direct γ-assay. ^{210}Pb activities were determined by accumulated counts at 46.5 keV, and ^{137}Cs activities by the counts at 662 keV. The ^{137}Cs activities were used to identify the Cs activity peaks of 1963 (atmospheric bomb fallout) and 1986 (Chernobyl accident). The decay curve of unsupported ^{210}Pb was used to estimate sedimentation rates since 1900.

Results and discussion

Seismic surveys

Figure 1 shows the bathymetry of the lake. The small bay in the south-western part of the lake differs from the main basin of the lake. It has shallow littoral slopes and a water depth that is generally less than 5 m. The main basin is characterized by very steep slopes in the south, more gentle slopes in the north, and a profundal region in which the water depth is $\sim$39 m. Oetheimer (1992) assumed that the small eastern basin is $\sim$20 m deep. The seismic surveys confirm this hypothesis and show roughly the dimensions of that basin (Figures 1 and 3).

In the deeper basin, the acoustic signal images 5–8 m of regularly layered sediment with lateral coherent seismic reflections (Figure 2). Seismic penetration, however, was partly masked, possibly by free gas, so that bedrock morphology could not be determined clearly. The layered sections lie above and below an intercalated unit characterized by chaotic/transparent seismic facies (Figure 2). This unit (Figure 2) is up to 2.5 m thick in the northern part of the central basin, thinning out towards the south. This unit is interpreted to be a mass-flow deposit with an interpolated volume of 113,000 m^3 (Figure 3) covering an area of $\sim 300 \times 150$ m with a maximum thickness of 250 cm. The lithology of the sediment cores refines the seismic findings and reveals that this unit is the proximal, debris flow-like part of an extensive mass-flow deposit. The distal part of the mass-flow can be tracked in the seismic data as a thinner unit (Figure 2) with a gradual upper transition to the overlying layered sediments. This unit can be mapped over the entire deep basin and coincides in the cores with much finer lithologies than those in the proximal parts. Seismic data also show that the mass-flow is homogenously covered by younger sediments, which are well-bedded and less than 1 m thick.

Sediment mineralogy

Detailed X-ray diffraction analyses of the sediment cores TOV01-5V and TOV01-6V show that they consist dominantly of dolomite. Minor components are calcite and quartz. The sediments clearly

represent the mineralogy of the bedrock in the catchment. No regeneration minerals from weathering of rocks or diagenesis processes were detected.

Sediment stratigraphy

Three piston cores (up to 734 cm sediment length) and 19 short gravity cores (up to 76 cm) were examined in detail in terms of their sedimentology. The locations of the coring sites are shown in Figure 1. Based on these 22 sediment cores, 4 main stratigraphical units and 5 sub-units can be distinguished. Two representative cores will be described here in detail (Figures 4 and 5). TOV01-8 and TOV01-6V were recovered in the northern basin, where the main part of the mass-flow was deposited. TOV01-7 and TOV01-5V are from the southern part of the main basin and consist of the distal mass-flow deposits. The topmost, post-event sediments from both gravity cores (TOV01-5V, −6V) were analyzed in detail. TOV01-5V and TOV01-6V were also used for isotopic dating (^{137}Cs, ^{210}Pb).

Unit 1

Unit 1 was recovered only in core TOV01-7 in the S of the lake basin and comprises 25 cm of gravel at the base and gravelly sand at the top (Figure 4). It is interpreted as the sediment deposited in the last stage of the proposed dead-ice body. The clay

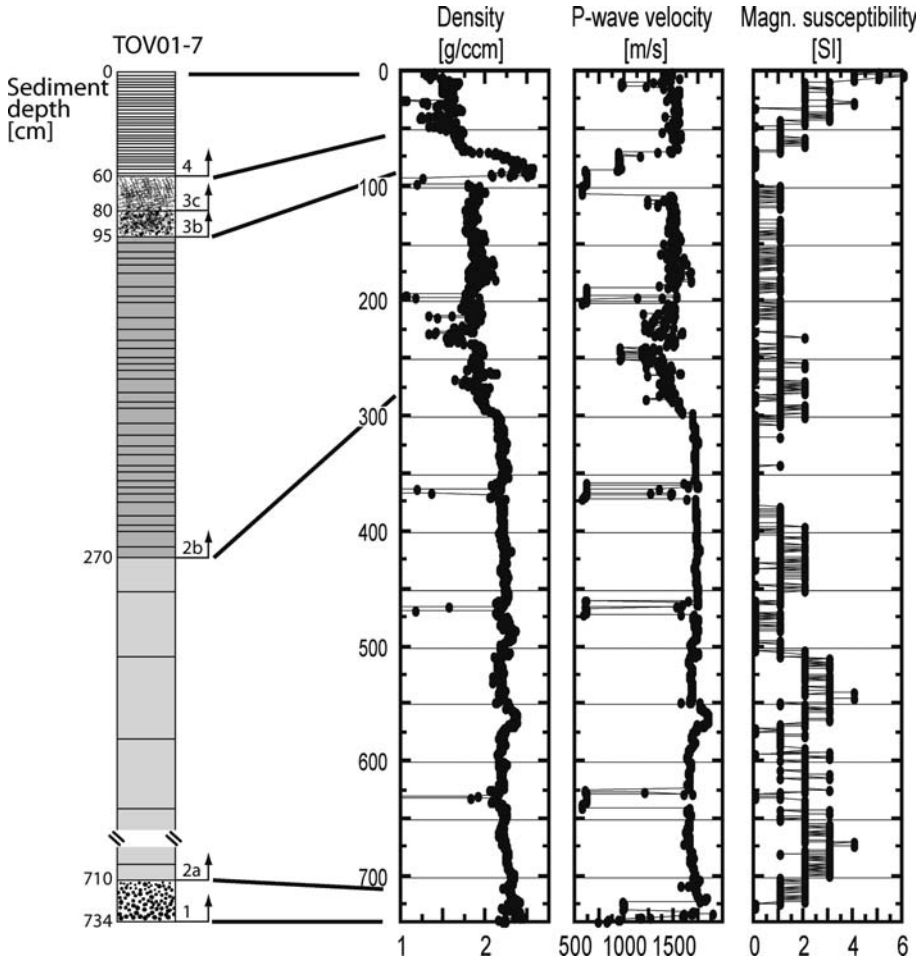

Figure 4. Sedimentology of core TOV01-7 from the southern part of the lake (distal part of the slump deposits) showing the following lithological units: 2a, carbonaceous ooze; 2b, stratified sediments; 3a, slump, stony grain sizes; 3b, slump, coarse grain sizes; 3c, slump, fine grain sizes; 4, laminated sediments. Also shown are the values of density, P-wave velocity, and magnetic susceptibility.

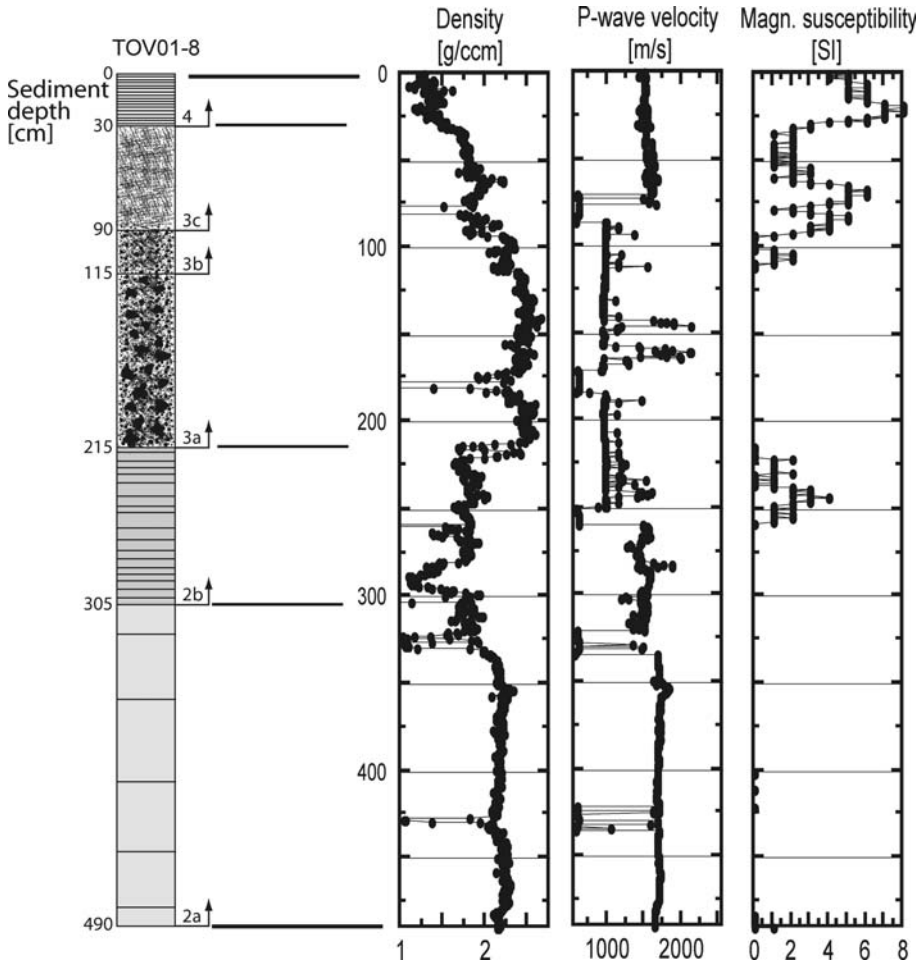

Figure 5. Sedimentology of core TOV01-8 from the northern part of the lake (proximal part of the slump deposits) showing the following lithological units: 1, gravelly sediments; 2a, carbonaceous ooze; 2b, stratified sediments; 3a, slump, stony grain sizes; 3b, slump, coarse grain sizes; 3c, slump, fine grain sizes; 4, laminated sediments. Also shown are the values of density, P-wave velocity, and magnetic susceptibility.

and silt grains were washed out in a high-energy system of water streams induced by the melting ice. The same mechanism has been described for the base-sediments of Soppensee, a post-dead-ice lake in central Switzerland (Sturm, unpublished data).

Unit 2

Unit 2 is divided into two sub-units, viz. 2a and 2b (Figures 4 and 5). A sharp boundary separates unit 1 from unit 2a in core TOV01-7. In both representative cores (TOV01-7, −8) the sediments of unit 2a consist of carbonaceous/dolomitic ooze, which is fine-grained and very stiff. The homogenous sediments vary in color from dark to light gray. They show high average values in P-wave velocity (~1700 m s^{-1}) and density (2.1 g cm^{-3}) with very little variation (Figure 5). The variation in magnetic susceptibility is also low. Unit 2a was recovered completely only in the core from the southern part of the lake (TOV01-7), and had a thickness of 440 cm. Unit 2a is interpreted as the initial lake sediment. The lake was in a pro-glacial position and the melt-water from the glacier was able to transport coarse sediments into the lake basin. We found no indication of soil formation and/or erosion in the catchment during this time period.

Unit 2b differs from unit 2a by having a generally lower P-wave velocity and a lower density

(Figures 4 and 5). This is caused by lithological changes: the sediment succession changes from a homogenous sediment to a well-stratified and sometimes laminated sediment with sand layers and organic-rich layers within the dolomite ooze. Additionally, some graded layers were observed that we interpret as the result of turbidity currents. Unit 2b is twice as thick in the very distal core TOV01-7 (185 cm) than in TOV01-8 (90 cm).

Unit 2b represents a time period with more ice-free areas in the catchment, resulting in more heterogeneous sedimentation than unit 2a with a coarser grain size and a higher organic carbon content, as well as single sand layers and layers of wood remains.

Unit 3

Unit 3 consists of much coarser sediment than the underlying and overlying units and is divided into three sub-units (Figures 4 and 5). Only core TOV01-8 shows the sediments of unit 3a. The sediments of this unit are 100 cm thick, consisting of gravel and stones up to 8 cm in diameter. Unit 3b, 25 cm thick in core TOV01-8 and 15 cm thick in core TOV01-7, is dominated by gravel that is finer than that in unit 3a. Fine grain size characterizes unit 3c in both cores. Sixty centimeter of unit 3c sediments were recovered in core TOV01-8 and 20 cm in core TOV01-7.

Unit 3 is interpreted to comprise the sediments of the mass-flow, which were also discernable from the seismic data. This mass-flow had a strong impact on the surface of the lake bottom, because a large volume of material (at least 113,000 m^3) was released into the central basin of the lake. Based on our age model (see below) and the large proportion of non-lacustrine components such as stones and gravel, we assume that the flow was triggered by the rock fall, which was dated by dendrochronolgy on rooted trunks in the lake to have occurred between winter 1597 and summer 1598 (Oetheimer 1992). The rock fall dammed the lake in the east, resulting in a doubling of the water depth to its modern value of 39 m. Another theory (Borsato, personal communication) assumes that the lake level rise was triggered by a continuously slow movement of debris down the slope of the hill rather than by a single short-term event. In fact, both theories would predict virtually the same effect on lake deposition and therefore do not change the interpretation of the mass-flow event as a time marker horizon for Lago di Tovel. Both scenarios would imply the clogging of the ancient outlet and the consequent damming of the lake, which would have resulted in a rapid increase in lake level and the formation of a new outlet. There is no doubt that the rising water level caused instabilities on the new lake slopes that finally released material into the lake by means of extensive mass-flow. Trees on the former shore died very soon after the lake rose, and the dating of the rooted tree trunks by Oetheimer (1992) provides valuable support for both theories. The seismically imaged flow deposit geometries and the investigation of the two piston cores from the northern (TOV01-8) and the southern (TOV01-7) parts of the lake, together with the results of the 27 gravity cores, indicate that the source of the mass-flow is the northern part of the lake. The thickness of the mass-flow sediment from the northern piston core, which even contains stones at its base, is almost 250 cm, whereas the thickness of the mass-flow sediments in the southern piston core is almost six times smaller (35 cm) and does not contain the proximal basal gravel unit (3a; Figures 4 and 5). In addition, unit 2b is twice as thick in the southern piston core as in the northern piston core. This agrees very well with a scenario involving mass-flow from the northern slope. The erosive energy of a mass-flow is much higher in proximal areas, where the slopes of the lake basin are steep, resulting in a high flow velocity. After sliding across the relatively horizontal lake basin, its energy, and therefore its erosive power, is much lower. Thus, we interpret the thinner layer of unit 2b in the northern part of the lake, in comparison to that in the southern part, as the result of erosion due to mass movement. This erosion can also be clearly seen on the seismic section that images the base of the mass-flow, where it cut and eroded the substrate, possibly deforming the underlying basin plain sediment (Figure 2), as has been observed in other lacustrine mass-flows (Schnellmann et al. 2002).

Unit 4

Unit 4 was recovered completely in every core from the profundal region of Lago di Tovel. This uppermost unit, covering the mass-flow unit lake-wide, consists of laminated silty sediment that can be correlated in detail with a resolution of up to 1 cm. The individual laminae consist of different

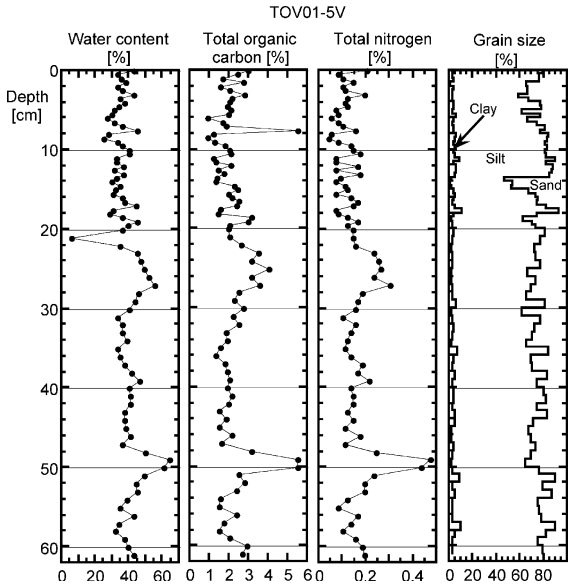

Figure 6. Sedimentological and geochemical parameters of TOV01-5V (distal part of the slump deposits).

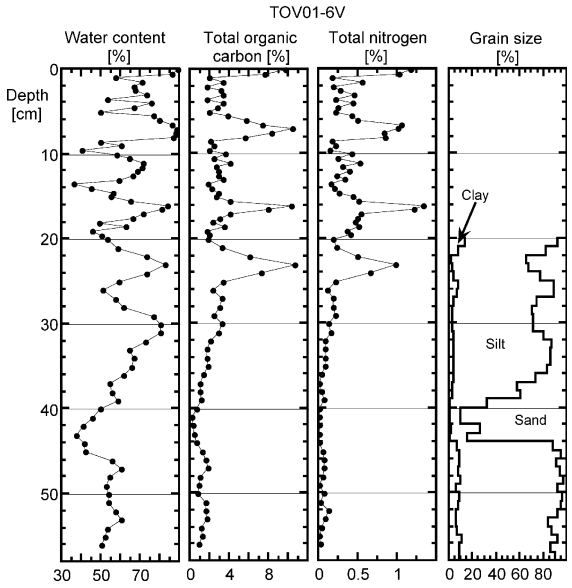

Figure 7. Sedimentological and geochemical parameters of TOV01-6V (proximal part of the slump deposits; grain sizes in the uppermost 20 cm of the core were not analyzed).

amounts of organic carbon and dolomite. Unit 4 shows the lowest values of P-wave velocity and density (Figures 4 and 5). Fine turbidite layers with a relatively high sand content were detected. Unit 4 is characterized by high-frequency variability in TOC, TN, and water content (Figures 6 and 7). The sediment thickness of unit 4 at every single core station depends on its proximity to the source of the mass-flow (e.g., TOV01-5V, −6V, see Figures 6 and 7), because the youngest sediment succession of unit 4 levels off the relief of the lake basin created by the mass-flow. The sediment thickness of unit 4 increases from 30 cm in the north to a maximum of 54 cm in the south. This kind of sediment represents a phase where the catchment has been stabilized after the rock fall/mass-flow event, resulting in a laminated layering of organic-rich layers and silty dolomite layers with tiny turbidity sand layers (Figures 6 and 7).

Dating and age model

The sediments of Lago di Tovel were dated using various different methods (Table 1). The rock fall is a time marker that was dated exactly by dendrochronology to have occurred in 1597/1598 AD (Oetheimer 1992). The thickness of the laminated post-mass-flow sediments varies between ~30 and ~54 cm depending on the vicinity of the coring position to the source of the landslide and the resulting bathymetric topography. Thus, the sedimentation rates vary between a minimum of 0.07 cm yr^{-1} in the southeastern part of the lake and a maximum of 0.18 cm yr^{-1} in the northern part. This inconsistency in the accumulation rates in different parts of the lake also affects the interpretation of the radiometric dating for the cores TOV01-5V, TOV01-6V, and TOV03-13 shown in Figures 8 and 9. The ^{137}Cs profiles of all three measured cores show a 1-peak curve instead of the general characteristic 2-peak curve. Additionally, the profile of TOV01-6V reaches its highest value in the topmost sample (Figure 8b).

Does the ^{137}Cs peak record the excessive bomb testing in 1963 or the Chernobyl accident in 1986? If the peak in the sediments of TOV01-5V and TOV03-13 (Figure 8a and c) belonged to 1963, the sedimentation rates would be slightly below the range calculated by the rock fall event of 1598 (0.05 and 0.06 cm yr^{-1}). Assuming that the ^{137}Cs peak belonged to 1986, the resulting calculated sedimentation rates of 0.12 and 0.13 cm yr^{-1} would agree well with the highest values calculated from the date of the mass-flow event. Taking into account that cores TOV01-5V and TOV03-13 are from areas with high sedimentation rates

Table 1. Comparison of sedimentation rates in Lago di Tovel determined from three sediment cores (TOV01-5V, TOV01-6V, and TOV03-13) and the 1597/1598 rock fall event.

Method	Core	Age (AD)	Sediment depth (cm)	Sedimentation rate (cm yr^{-1})
Rock fall/dendrochronology	All	1597/1598	30–54	0.07–0.13
^{137}Cs	TOV01-5V	1986	1.5–2	0.12
^{137}Cs	TOV01-5V	1963	1.5–2	0.05
^{137}Cs	TOV01-6V	?	Core top	?
^{137}Cs	TOV03-13	1986	2–2.5	0.13
^{137}Cs	TOV03-13	1963	2–2.5	0.06
^{210}Pb	TOV01-5V		0–11.5	0.18
^{210}Pb	TOV01-6V		0–9	0.09
^{210}Pb	TOV03-13		0–11	0.18
^{210}Pb CRS-model	TOV03-13		0–11	0.08

(e.g., TOV03-13: 0.13 cm yr^{-1}), it is likely that the ^{137}Cs peak in TOV01-5V and TOV03-13 indeed marks the Chernobyl accident in 1986 (Figure 8a and c) and not the atmospheric bomb tests of 1963. The lack of a second peak might be due to the very high concentration of ^{137}Cs in the topmost samples masking the older and therefore smaller peak from 1963. Additionally, sampling intervals of 0.5 cm correspond to a time period of ~4–7 years. The $^{137}Cs/^{210}Pb$ U(unsupported) activity ratios clearly show a second peak at 3.5–4 cm for cores TOV01-5V and TOV03-13, which reflect the atmospheric bomb-test maximum in 1963 (Figure 9). There is no distinct second peak in the sediments of TV01-6V, but a higher activity ratio in 1–1.5 cm might be an equivalent to that.

The ^{210}Pb data from TOV01-5V and TOV03-13 suggest higher sedimentation rates (0.18 cm yr^{-1} in both cases) than those calculated using either of the other methods. They are considered to be uncertain because the decrease in ^{210}Pb activity within the uppermost two samples from TOV03-13 is unusual (Figures 8a,c). Additionally, the ^{210}Pb dating of the two cores overestimates the sedimentation rates possibly because a small change in the gradient of the steep slope from the straight line of the ^{210}Pb data would have a big influence on the resulting sedimentation rates. Moreover, one could use a different gradient for the uppermost 2–4 cm of TOV01-6V and TOV03-13. Nonetheless the ^{210}Pb dating also indicates that the ^{137}Cs peak belongs to 1986.

The non-monotonic variations in ^{210}Pb activities precluded use of the Constant Initial Concentration (CIC) model. We therefore applied the Constant Rate of Supply (CRS) model (Appleby and Oldfield 1978; Appleby 2001) to the ^{210}Pb profiles, e.g., to TOV03-13 (Figure 9). The CRS calculation shows good agreement with the ^{137}Cs measurements (Figure 9), clearly indicating that the ^{137}Cs peak records the Chernobyl fallout in 1986. The model also suggests a period of rapid sedimentation ~50 years ago, which is in good agreement with the lithology, where a fining upward sequence (sand to clay) was sedimented between 4 and 5.5 cm.

In conclusion, the sedimentation rates calculated from the date of the mass-flow are very reliable. They range between 0.07 and 0.13 cm yr^{-1}, depending on the lake bottom morphology after the landslide event.

Conclusion

Based on a preceding seismic survey, a total of 27 gravity cores and 3 piston cores were taken in Lago di Tovel in 2001 and 2003. The investigation of the sediments revealed a complex sedimentation history within this lake basin. In 1597/1598 a major rock fall altered the sedimentation conditions completely and led almost to a doubling of the water depth. It triggered a huge mass-flow in the northern part of the lake that was deposited over the entire deep basin.

The newly acquired bathymetric map reveals a 39 m deep central lake basin with steep slopes to the north and to the south. In the east of the main basin, separated from it by a small sill, exists another small sub-basin. Results of a seismic survey and detailed analyses of the sediment cores revealed the existence of mass-flow deposits with a maximum thickness of 2.5 m in the northern part of the lake and 50 cm in the southern part. In

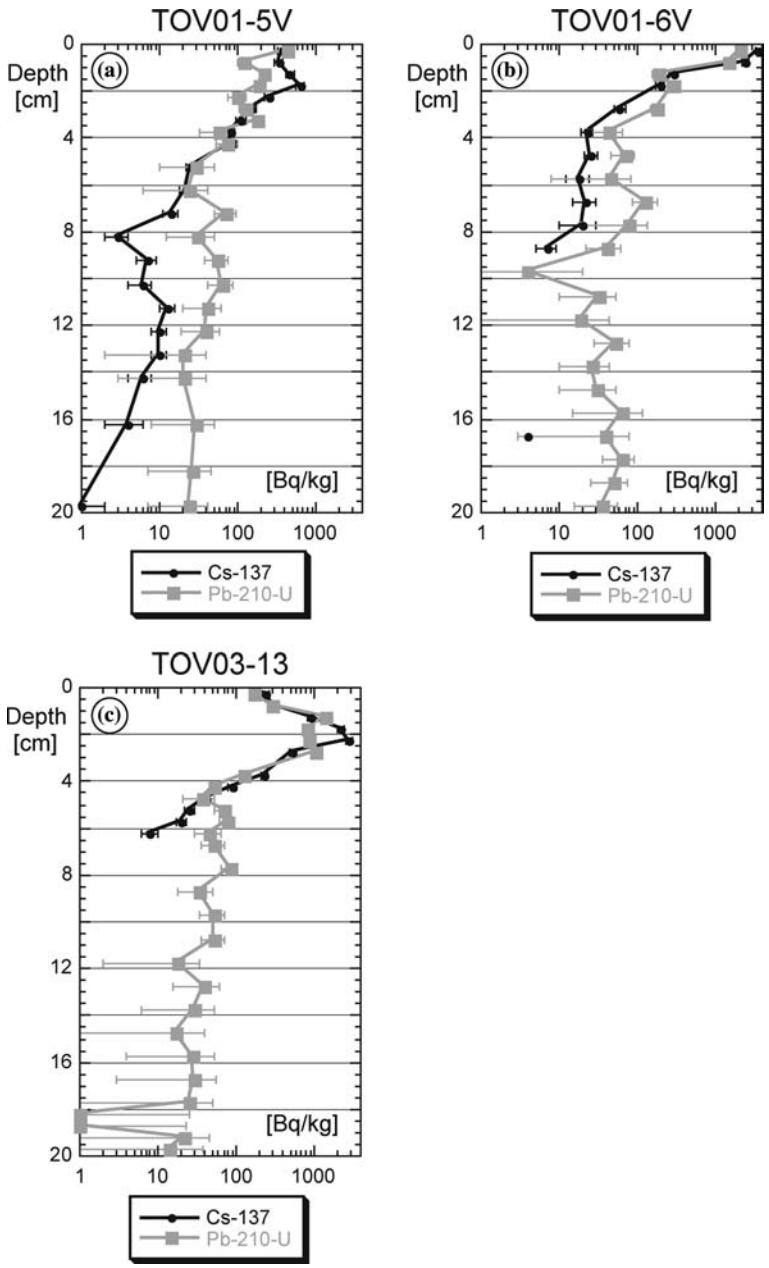

Figure 8. Profiles of fallout activities of unsupported ^{210}Pb and of ^{137}Cs in sediment cores from the deepest part of Lago di Tovel. (a) TOV01-5V (distal part of the slump deposits). (b) TOV01-6V (proximal part of the slump deposits). (c) TOV03-13 (distal part of the slump deposits).

accordance with the mass-flow geometry, the sediments are much coarser in the north than in the south. The event is a consequence of slope instabilities caused by the water level rising from ~20 to 39 m.

Sedimentation in Lago di Tovel is generally characterized by dead-ice/pro-glacial sediments, mass-flow sedimentation, regular run-off sedimentation from the catchment, and autochthonous bio-productivity. Sedimentation rates based on dating using ^{210}Pb, ^{137}Cs, the CRS model, and dendrochronology, show very heterogeneous values within this small lake, ranging from 0.07 to 0.18 cm yr^{-1}. The ^{137}Cs peak recorded in the

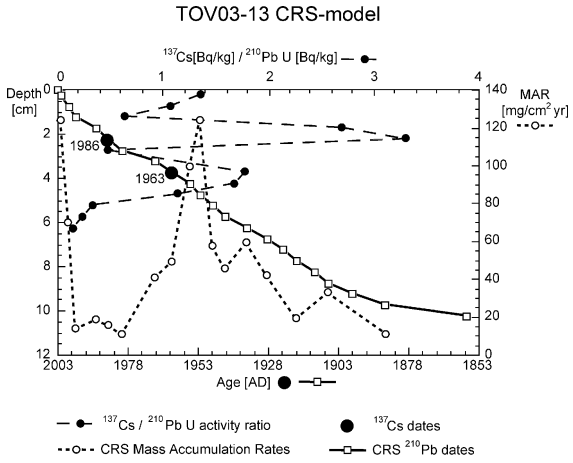

Figure 9. Radiometric age model of TOV03-13 showing the CRS model dates and mass accumulation rates (MAR), the 1986 and 1963 fallout maxima determined from the ^{137}Cs measurements, and the profile of the ^{137}Cs/^{210}Pb U (unsupported) activity ratio.

sediment cores was caused by fallout after the Chernobyl accident. ^{137}Cs/^{210}Pb activity ratios revealed the bomb-testing peak of 1963, and all ^{137}Cs dates are in good agreement with the ^{210}Pb chronology.

The stable and permanent meromixis of the oligotrophic lake, which existed even before the doubling of the water depth, is likely to have been caused by a combination of its topographic setting (mountainous landscape) and a five-month period of ice cover. Both shield the water body from stormy winds in spring and autumn.

Even during the pre-rockfall time periods, the sediments were laminated and stratified when the lake was half as deep as it is now. Analyses of the modern and ancient sediments of Lago di Tovel lead to the assumption that the lake was always meromictic even before the lake level rise. This is in accordance with the meromixis of the modern lake (Oetheimer 1992; Corradini et al. 2001).

Especially in small lakes, there is a tendency to base paleoenvironmental reconstructions on proxy data derived from very few sediment cores, or in the worst case even from one single core. The validity of this approach rests on the assumption that the final horizontal distribution of sedimenting material is influenced only by the funnel effect (Ohle, 1962). Our studies on Lago di Tovel demonstrate that this is a risky assumption that can lead to serious misinterpretation of the results. The sediments of small lakes can have a complex structure. In the case of small alpine lakes, with a catchment area spanning a large altitude range, the resulting enhanced structural complexity makes multiple coring an absolute necessity if serious errors in interpretation are to be avoided.

Acknowledgements

The seismic survey was conducted with the help of Katrin Monecke from the Limnogeology Laboratory of the Geological Institute of ETH Zürich. We would like to express our thanks to Ingrid Holderegger, Yvonne Lehnhard, Brian Sinnet, Lydia Zweifel, Alois Zwyssig (all at EAWAG), Piero Guilizzoni, Andrea Lami (both at CNR Hydrobiological Institute, Verbania-Pallanza), Daniel Spitale, Massimiliano Tardio, Nicola Angeli (all at The Museum of Natural Science, Trento), Christian Ohlendorf (GEOPOLOAR, University of Bremen), Richard Niederreiter and his co-workers (UWITEC) for their help during the field work, laboratory work, and the sediment sampling, and Peter Appleby for fruitful discussions on the dating results. This study was financed by the Autonomous Province of Trento, Italy, within the multidisciplinary project BEST (Blooms and Environment: Science for Tovel), and by EAWAG.

References

Agustí-Panareda A. and Thompson R. 2002. Reconstructing air temperature at eleven remote alpine and arctic lakes in Europe from 1781 to 1997 AD. J. Paleolimnol. 28: 7–23.

Appleby P.G. 2001. Chronostratigraphic techniques in recent sediments. In: Last W.M. and Smol J.P. (eds), Tracking Environmental Change Using Lake Sediments, Vol. 1. Kluwer Academic Publishers, Dordrecht, The Netherlands, pp. 171–203.

Appleby P.G. and Oldfield F. 1978. The calculation of ^{210}Pb data from sites with varying sediment accumulation rates. Hydrobiologia 214: 35–42.

Baldi E. 1941. Ricerche idrobiologiche sul lago di Tovel. Mem. Mus. St. Nat. Ven. Tr. 6: 1–297.

Battarbee R.W., Grytnes J.-A.R.T., Appleby P.G., Catalan J., Korhola A., Birks H.J.B., Heegaard E. and Lami A. 2002. Comparing palaeolimnological and instrumental evidence of climate change for remote mountain lakes over the last 200 years. J. Paleolimnol. 28: 161–179.

Biondi E., Pedrotti F. and Tomasi G. 1981. Relitti di antiche foreste sul fondo di alcuni laghi del Trentino. Studi Trentino di Scienze Naturai, Acta Biologica 58: 93–117.

Bradley R.S., Briffa K.R., Cole J., Hughes M.K. and Osborn T.J. 2003. The climate of the last millennium. In Alverson K., Bradley R.S. and Pedersen T.F. (eds), Paleoclimate, Global Change and the Future. Springer-Verlag, Berlin, pp. 105–141.

Cantonati M., Tardio M., Tolotti M. and Corradini F. 2003. Blooms of the dinoflagellate *Glenodinium sanguineum* obtained during enclosure experiments in lake Tovel (N. Italy). J. Limnol. 62: 79–87.

Cordella P., Miola A., Trevisan R., Cappelletti E.M. and Paganelli A. 1980. Concentrazioni di fosforo e di azoto inorganico in tre laghi del Nord Italia. In: Zara (ed.), Atti I Congresso Nazionale della Società Italiana di Ecologia, Salsomaggiore Terme (PR), pp. 117–121.

Corradini F., Flaim G. and Pinamonti V. 2001. Five years of limnological observations on lake Tovel (1995–1999): some considerations and comparisons with data. Atti Associazione Italiana Oceanologia Limnologia 14: 209–218.

Dodge J.D. 1970. Report of limnological investigation of lake Tovel (Trentino – N. Italy). St. Trent. Sci. Nat. 47: 91–94.

Freshfield D.W. 1875. Italian Alps: Sketches in the Mountains of Ticino, Lombardy, the Trentino, and Venetia. Longmans, Green, and Co., London, 385pp.

Fuganti A. and Morteani G. 1999. La storia del Lago di Tovel in base ai sedimenti della Baia Rossa (Trentino). Geologia Tecnica and Ambientale 3: 21–32.

Lami A., Guilizzoni P. and Masaferro J. 1991. Record of fossil pigments in an alpine lake (L. Tovel, N. Italy). Mem. Ist. Ital. Idrobiol. 49: 117–126.

Marchesoni V. 1941. Sulla posizione sistematica del *Glenodinium sanguineum* March. determinante l'arrossamento del Lago di Tovel. Studi Trentino di Scienze Naturai 1: 11–18.

Oetheimer C. 1992. La foresta sommersa del Lago di Tovel (Trentino): reinterpretazione e datazione dendrocronologica. Studi Trentino di Scienze Naturai 67: 3–23.

Ohle W. 1962. Der Stoffhaushalt der Seen als Grundlage einer allgemeinen Stoffwechseldynamik der Gewässer. Kieler Meeresforschungen 18: 107–120.

Ohlendorf C., Sturm M. and Hausmann S. 2003. Natural environmental changes and human impact reflected in sediments of a high Alpine lake in Switzerland. J. Paleolimnol. 30: 297–306.

Paganelli A. 1992. Lake Tovel (Trentino): limnological and hydrobiological aspects. Mem. Ist. Ital. Idrobiol. 50: 225–257.

Paganelli A., Cordella P., Trevisian R. and Cappelletti E.M. 1980. Il Lago di Tovel (Trento) e sue modificazioni ambientali. In: Zara (ed.), Proc. Congr. Naz. Soc. It. Ecolog., pp. 87–93.

Paganelli A., Miola A. and Cordella P. 1988. Il Lago di Tovel (Trentino) e la circolazione delle sue acque. Riv. di Idrobiol. 27: 363–376.

Perini Aregger S.E. 1968. Tovel (TN), un patrimonio di alghe. Italia Nostra, Roma 60: 92–93.

Schnellmann M., Anselmetti F.S., Giardini D., McKenzie J.A. and Ward S. 2002. Prehistoric earthquake history revealed by lacustrine slump deposits. Geology 30: 1131–1134.

Sturm M., Kulbe T. and Ohlendorf C. 2003. Archives in the depths of high mountain lakes. EAWAG News 55e: 15–17.

Zolitschka B., Mingram J., van der Gaast S., Jansen J.H.F. and Naumann R. 2001. Sediment logging techniques. In: Last W.M. and Smol J.P. (eds), Tracking Environmental Change Using Lake Sediments, Vol. 1. Kluwer Academic Press, Dordrecht, The Netherlands, pp. 137–153.